

Revisiting the anomalous spin-Hall effect of light near the Brewster angle

Xiaohui Ling^{1,2,*}, Weilai Xiao¹, Shizhen Chen,³ Xinxing Zhou⁴, Hailu Luo³, and Lei Zhou^{2,†}

¹College of Physics and Electronic Engineering, Hengyang Normal University, Hengyang 421002, China

²State Key Laboratory of Surface Physics, Key Laboratory of Micro and Nano Photonic Structures (Ministry of Education) and Physics Department, Fudan University, Shanghai 200433, China

³Laboratory for Spin Photonics, School of Physics and Electronics, Hunan University, Changsha 410082, China

⁴Key Laboratory of Low-Dimensional Quantum Structures and Quantum Control of Ministry of Education, Synergetic Innovation Center for Quantum Effects and Applications, School of Physics and Electronics, Hunan Normal University, Changsha 410081, China



(Received 18 November 2020; revised 11 February 2021; accepted 5 March 2021; published 22 March 2021)

Optical spin-Hall effect (SHE) exhibits many intriguing features as a linearly polarized (LP) light beam strikes an interface at incident angles around the Brewster angle, but the underlying physics remains obscure. Here, we elucidate the physics through reanalyzing this problem employing rigorous calculations and the Berry phase concept. As a circularly polarized (CP) light beam strikes an optical interface, the reflected light beam contains two components, a spin-flipped abnormal mode acquiring geometric phases (thus exhibiting a spin-Hall shift) and a spin-maintained normal mode without such phases. Strengths of these two modes are determined by the incident angle and the optical properties of the interface. Under the LP incidence, however, a spin component inside the reflected light beam must be the sum of normal and abnormal components of reflected light beams corresponding to CP incidences with different helicity, which thus sensitively depends on the incident angle. In particular, at incident angles near the Brewster one, reflection coefficients for two CP components exhibit opposite signs, leading to significant destructive interferences between normal and abnormal modes, finally generating highly deformed reflected light patterns with anomalously enhanced spin-Hall shifts. These findings can be extended to both reflected and transmitted cases with Brewster-like behaviors. Our analyses reinterpret previously discovered effects, providing an alternative understanding on the SHE of light.

DOI: [10.1103/PhysRevA.103.033515](https://doi.org/10.1103/PhysRevA.103.033515)

I. INTRODUCTION

Light reflection can vanish as a p -polarized light strikes a dielectric interface at a particular incident angle, known as the Brewster angle [1,2]. Such a property was widely used to polarize the incident light. For light beams composed by plane waves with different wave vectors, many intriguing effects were discovered as such beams strike an optical interface at the Brewster angle, such as cross polarization conversion [3–5] and the generations of vectorial vortex beams [6,7]. Recently, much attention was denoted to studying the spin-Hall effect (SHE) of light [8–14] as a linearly polarized (LP) light beam is reflected by an optical interface at incident angles around the Brewster angle. Many unusual features of SHE were discovered in such an optical process. For example, the spin-Hall shifts of light beams are anomalously enhanced as the incident angle approaches the Brewster angle, and spin-polarized reflected light beams exhibit highly deformed transverse patterns [15–25]. The SHE of light in many materials or interfaces with Brewster-like or pseudo-Brewster angles has been widely studied [26–31] and utilized for precise metrology and sensing [32–36].

Many theoretical efforts have been devoted to understanding the nature of SHE of light at sharp interfaces, including the cases at Brewster angles. In 2004, Onoda *et al.* [8] extended the semiclassical theory of SHE of electrons to study the optical SHE. Such a theory omits the wave nature of light, which was soon refined by Bliokh *et al.* [9,10] in 2006 who proposed a more accurate wave theory. The wave theory, based on decompositions of light beams to LP plane waves, can well reproduce the anomalous SHEs discovered for reflected beams at the Brewster angles [15–19]. However, the underlying physics accounting for such unusual effects were not clearly explained, but are rather simply attributed to the enhanced spin-orbit interactions in such special cases. Later, Ren *et al.* re-examined such a process [20] based on circularly polarized (CP) bases, and pointed out that the spin-Hall shifts discovered under LP incidence are weighted averages of results obtained under CP incidences with different spins. However, the underlying physics, such as why and how the coherent superposition of two CP modes can lead to such unusual effects in such special cases, are still not well elucidated.

In this paper, we revisit this problem based on rigorous calculations in CP bases and the Berry-phase concept. As a CP light beam illuminates an optical interface, we find that the reflected beam generally contains two parts, which are normal and abnormal modes with spin (helicity) conserved and reversed, respectively. Whereas the abnormal mode exhibits a spin-dependent Pancharatnam-Berry phase which can

*xhling@hynu.edu.cn

†phzhou@fudan.edu.cn

generate a SHE, the normal mode does not acquire any such additional phases. Meanwhile, the coefficients of these two terms are determined by the Fresnel's coefficients at this optical interface, which, in turn, sensitively depend on the incident angle and the material properties. Therefore, a spin component inside the reflected beam under an LP incidence is the sum of normal and abnormal modes corresponding to CP incidences with opposite spins, respectively. Interference between these two modes generates fascinating properties discovered in previous calculations in LP bases. In particular, at the vicinities of Brewster-angle incidence, Fresnel's coefficients of two polarizations are opposite leading to destructive interferences between two modes, which significantly deforms the field pattern and abnormally enlarge the spin-Hall shift of the resultant beam. We finally extend our ideas to both reflection and transmission cases with Brewster-like behaviors.

II. THEORY OF LIGHT BEAM REFLECTED AT SHARP INTERFACES

The light beam reflected at an optical interface is a coherent superposition of reflected plane waves inside the beam. We define (x, y, z) and (x^a, y^a, z^a) as the laboratory and local coordinate systems, respectively, where y and y^a point to the same direction and z^a is parallel to the propagation direction of the beam [Fig. 1(a)]. Here, the superscripts $a = \{i, r\}$ label the incident and reflected light, respectively. Based on the angular spectrum theory, we can expand the incident or reflected beam as linear combinations of plane waves in the CP basis,

$$\mathbf{E}^a(\mathbf{r}^a) = \int d^2\mathbf{k}_\perp^a e^{i\mathbf{k}_\perp^a \cdot \mathbf{r}^a} [u_+^a(\mathbf{k}^a)\hat{\mathbf{v}}_+(\mathbf{k}^a) + u_-^a(\mathbf{k}^a)\hat{\mathbf{v}}_-(\mathbf{k}^a)], \quad (1)$$

where $\mathbf{k}^a \cdot \mathbf{r}^a = \mathbf{k}_\perp^a \cdot \mathbf{r}_\perp^a + k_z^a z^a$ with $k_z^a = \sqrt{(k^a)^2 - (k_\perp^a)^2}$, \mathbf{r}_\perp^a and \mathbf{k}_\perp^a are the wave vector and position vector in the local coordinate, $\hat{\mathbf{v}}_\sigma(\mathbf{k}^a) = [\hat{\mathbf{v}}_p(\mathbf{k}^a) + i\sigma\hat{\mathbf{v}}_s(\mathbf{k}^a)]/\sqrt{2}$ ($\sigma \in \{+, -\}$) denote the unit vectors of left (+) and right (-) CPs with $\hat{\mathbf{v}}_s(\mathbf{k}^a) = \hat{\mathbf{z}} \times \mathbf{k}^a/|\hat{\mathbf{z}} \times \mathbf{k}^a|$ and $\hat{\mathbf{v}}_p(\mathbf{k}^a) = \hat{\mathbf{v}}_s^a \times \mathbf{k}^a/k^a$ being the unit polarization vectors of s -polarized and p -polarized plane waves defined in the laboratory coordinate, and $u_\pm^a(\mathbf{k}^a)$ are the expansion coefficients. Directions of these beams θ_K^a are dictated by the wave vectors \mathbf{K}^a of the central plane waves

and directions of different plane waves are represented by ϑ_k^a [Fig. 1(b)].

For the present reflection problem, we have

$$\begin{aligned} \begin{pmatrix} u_+^r(\mathbf{k}^r) \\ u_-^r(\mathbf{k}^r) \end{pmatrix} &= \mathbf{R}(\mathbf{k}_\parallel) \begin{pmatrix} u_+^i(\mathbf{k}^i) \\ u_-^i(\mathbf{k}^i) \end{pmatrix} \\ &= \begin{bmatrix} r_{++}(\mathbf{k}_\parallel) & r_{+-}(\mathbf{k}_\parallel) \\ r_{-+}(\mathbf{k}_\parallel) & r_{--}(\mathbf{k}_\parallel) \end{bmatrix} \begin{pmatrix} u_+^i(\mathbf{k}^i) \\ u_-^i(\mathbf{k}^i) \end{pmatrix} \end{aligned} \quad (2)$$

to connect $u_\pm^r(\mathbf{k}^r)$ and $u_\pm^i(\mathbf{k}^i)$ with \mathbf{k}^r and \mathbf{k}^i interconnected by Snell's law. Here $r_{++}(\mathbf{k}_\parallel) = r_{--}(\mathbf{k}_\parallel) = [r_p(\mathbf{k}_\parallel) + r_s(\mathbf{k}_\parallel)]/2$ and $r_{+-}(\mathbf{k}_\parallel) = r_{-+}(\mathbf{k}_\parallel) = [r_p(\mathbf{k}_\parallel) - r_s(\mathbf{k}_\parallel)]/2$ are Fresnel reflection coefficients of CP waves with tangential wave vector \mathbf{k}_\parallel defined in the laboratory coordinate system, where $r_p(\mathbf{k}_\parallel)$ and $r_s(\mathbf{k}_\parallel)$ are, respectively, Fresnel reflection coefficients of p - and s -polarized plane waves within the beam. At an interface between two isotropic dielectrics, these coefficients are derived based on the amplitude ratio of reflected and incident electric fields [1], i.e.,

$$r_p(\mathbf{k}_\parallel) = \frac{k_z^{(2)}n_1^2 - k_z^{(1)}n_2^2}{k_z^{(1)}n_2^2 + k_z^{(2)}n_1^2}, \quad r_s(\mathbf{k}_\parallel) = \frac{k_z^{(1)} - k_z^{(2)}}{k_z^{(1)} + k_z^{(2)}}, \quad (3)$$

where $k_z^{(1)} = k^i \cos \vartheta_k^i$, $k_z^{(2)} = k^r \cos \vartheta_k^r$, $n_{1,2}$ are refractive indices of the two media on two sides of the interface, $\vartheta_k^i = \sin^{-1}[n_1 \sin \vartheta_k^i/n_2]$, $k^i = n_1 k_0$, $k^r = n_2 k_0$, and $k_0 = 2\pi/\lambda$ is the free-space wave number.

To benefit further calculations, we rewrite the \mathbf{E} -field distributions of the light beams on reference planes defined with $z^a = \text{const.}$ as

$$\mathbf{E}_\perp^a(\mathbf{r}_\perp^a, z^a) = \int d^2\mathbf{k}_\perp^a e^{i\mathbf{k}_\perp^a \cdot \mathbf{r}_\perp^a} [U_+^a(\mathbf{k}^a)\hat{\mathbf{V}}_+ + U_-^a(\mathbf{k}^a)\hat{\mathbf{V}}_-], \quad (4)$$

where all wave components are assumed to take identical spin vectors of the central \mathbf{K}^a vector and $\hat{\mathbf{V}}_\sigma(\mathbf{K}^a) = (\hat{\mathbf{x}}^a + i\sigma\hat{\mathbf{y}}^a)/\sqrt{2}$. Here, $U_\pm^a(\mathbf{k}^a)$ are related to $u_\pm^a(\mathbf{k}^a)$ defined in Eq. (1) via

$$\begin{pmatrix} U_+^a(\mathbf{k}^a) \\ U_-^a(\mathbf{k}^a) \end{pmatrix} = \mathbf{P}^{(a)} \begin{pmatrix} u_+^a(\mathbf{k}^a) \\ u_-^a(\mathbf{k}^a) \end{pmatrix}, \quad (5)$$

where $P_{\sigma\sigma'}^{(a)} = [\hat{\mathbf{V}}_{\sigma'}(\mathbf{K}^a)]^* \cdot \hat{\mathbf{v}}_\sigma(\mathbf{k}^a)$ ($\sigma, \sigma' \in \{+, -\}$) are the elements of $\mathbf{P}^{(a)}$, representing a projection between spin vectors of a plane wave with \mathbf{k}^a and the center one \mathbf{K}^a . Combining

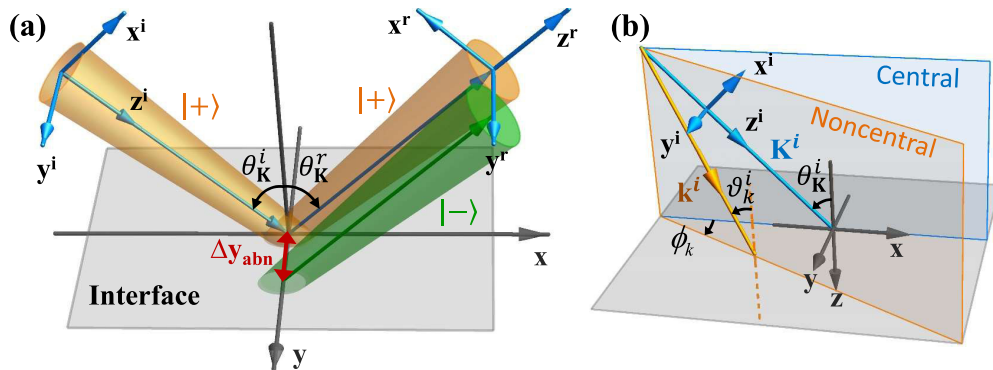


FIG. 1. Schematic of a spin-polarized light beam reflected at a single interface (say, air-glass interface). (a) The reflected beam consists of a spin-reversal mode with a transverse spin-Hall shift Δy_{abn} and a spin-maintained mode without shifts. (b) Schematics of incident planes of the central (\mathbf{K}^i) and noncentral (\mathbf{k}^i) plane waves within the incident beam. Here $|+\rangle$ and $|-\rangle$ represent left- and right-handed CPs, respectively.

Eqs. (2) and (5), we finally get

$$\begin{bmatrix} U_+^r(\mathbf{k}^r) \\ U_-^r(\mathbf{k}^r) \end{bmatrix} = \mathbf{M}^{(r)} \begin{bmatrix} U_+^i(\mathbf{k}^i) \\ U_-^i(\mathbf{k}^i) \end{bmatrix}, \quad (6)$$

where $\mathbf{M}^{(r)} = \mathbf{P}^{(r)} \cdot \mathbf{R}(\mathbf{k}_{\parallel}) \cdot (\mathbf{P}^{(i)})^{-1}$ whose elements are

$$\begin{aligned} M_{++} &= M_{--}^* = [A^r (B^i)^* r_p(\mathbf{k}_{\parallel}) + (A^i)^* B^r r_s(\mathbf{k}_{\parallel})] / C^i \\ M_{+-} &= M_{-+}^* = [A^r B^i r_p(\mathbf{k}_{\parallel}) - A^i B^r r_s(\mathbf{k}_{\parallel})] / C^i. \end{aligned} \quad (7)$$

Here, $A^a = \cos \vartheta_k^a (\cos \phi_k \cos \theta_{\mathbf{k}}^a - i \sin \phi_k) + \sin \vartheta_k^a \sin \theta_{\mathbf{k}}^a$, $B^a = \cos \phi_k - i \cos \theta_{\mathbf{k}}^a \sin \phi_k$, and $C^i = A^i (B^i)^* + (A^i)^* B^i$ with ϕ_k and ϑ_k^a defined in Fig. 1(b) (see Appendix A for a detailed derivation). Note that Eq. (6) connects $U_{\pm}^r(\mathbf{k}^r)$ with $U_{\pm}^i(\mathbf{k}^i)$, which dictates the transverse patterns in the k space of the reflected and incident beams, respectively [see Eq. (4)].

Assume that the incident beam is a left-handed CP Gaussian one with \mathbf{E} -field distribution on its waist plane being

$$\mathbf{E}_+^i(\mathbf{r}_{\perp}^i) = \exp[-(r_{\perp}^i/w_0)^2] \hat{\mathbf{V}}_+^i, \quad (8)$$

with w_0 being the half width of the beam waist; we find that $U_+^i(\mathbf{k}^i) = \frac{w_0^2}{2} \exp[-(k_{\perp}^i w_0)^2/4]$ and $U_-^i(\mathbf{k}^i) \equiv 0$. Putting $U_{\pm}^i(\mathbf{k}^i)$ into Eq. (6) to get $U_{\pm}^r(\mathbf{k}^r)$, we finally get the reflected \mathbf{E} fields as

$$\begin{aligned} E_{++}^r(\mathbf{r}_{\perp}^r) &= \int d^2 \mathbf{k}_{\perp}^r e^{i \mathbf{k}^r \cdot \mathbf{r}^r} M_{++} U_+^i(\mathbf{k}^i) \\ E_{-+}^r(\mathbf{r}_{\perp}^r) &= \int d^2 \mathbf{k}_{\perp}^r e^{i \mathbf{k}^r \cdot \mathbf{r}^r} M_{-+} U_+^i(\mathbf{k}^i). \end{aligned} \quad (9)$$

Here, the spin-maintained and spin-reversal beams are referred to as normal and abnormal modes, respectively. This means that even though the incident beam exhibits a pure spin, the reflected beam can still contain a spin-reversal abnormal component which comes from the ‘‘effective anisotropy’’ possessed by the optical interface at oblique incidence [i.e., $r_{+-} = (r_p - r_s)/2 \neq 0$]. When the incident beam is a right-handed CP one, we can also obtain the normal and abnormal modes in the reflection, i.e., $E_{--}^r(\mathbf{r}_{\perp}^r)$ and $E_{-+}^r(\mathbf{r}_{\perp}^r)$, akin to Eq. (9).

Finally, with the \mathbf{E} -field distribution of the reflected beam fully known, we can then use the following formula:

$$\Delta y = \frac{\iint y^r |\mathbf{E}|^2 dx^r dy^r}{\iint |\mathbf{E}|^2 dx^r dy^r}, \quad (10)$$

to calculate the spin-Hall shift of a light beam.

III. GEOMETRIC BERRY PHASE AND ANGULAR MOMENTUM CONSERVATION

To further analyze the underlying physics, we re-examine the matrices $\mathbf{P}^{(a)}$ and $\mathbf{M}^{(r)}$ under the paraxial-wave approximation. Based on such an approximation, we have $\vartheta_k^a \approx \theta_{\mathbf{k}}^a$, $\cos \phi_k \approx 1$, and $\sin \phi_k \approx \phi_k \approx k_y / (k_0 \sin \theta_{\mathbf{k}}^a)$, and thus $A^a \approx B^a \approx 1 - i \phi_k \cos \theta_{\mathbf{k}}^a \approx \exp(-i \phi_k \cos \theta_{\mathbf{k}}^a)$. Therefore, the matrix $\mathbf{P}^{(a)}$ now reads (see Appendix B)

$$\mathbf{P}^{(a)} \approx \begin{bmatrix} \exp(i \Phi_+^a) & 0 \\ 0 & \exp(i \Phi_-^a) \end{bmatrix}, \quad (11)$$

where $\Phi_{\sigma}^a = -\sigma^a \cos \theta_{\mathbf{k}}^a \cdot \phi_k \approx -\sigma^a k_y \cos \theta_{\mathbf{k}}^a / (k_0 \sin \theta_{\mathbf{k}}^a)$ ($\sigma^a \in \{+, -\}$) is a k_y -dependent geometric phase originated from the projection operation between the polarization vector

of the central plane wave and the noncentral ones inside the beam. Note that $\sigma_z = \sigma^a \cos \theta_{\mathbf{k}}^a$ is the projection of the spin of the beam in the laboratory z direction and ϕ_k is the rotation of the azimuthal angle of the incident plane [Fig. 1(b)], and thus Φ_{σ}^a reflects the coupling between spin (σ_z) and local rotation (ϕ_k) of the polarization vectors of each plane wave. Hence, Φ_{σ}^a can be seen as a spin-redirected Berry phase [12,13,37].

With the $\mathbf{P}^{(a)}$ matrix known, we further simplify the $\mathbf{M}^{(r)}$ matrix defined in Eq. (6) as

$$\mathbf{M}^{(r)} \approx \begin{bmatrix} r_{++}(\mathbf{k}_{\parallel}) & r_{+-}(\mathbf{k}_{\parallel}) \exp(i \Phi_+^{\text{abn}}) \\ r_{-+}(\mathbf{k}_{\parallel}) \exp(i \Phi_-^{\text{abn}}) & r_{--}(\mathbf{k}_{\parallel}) \end{bmatrix}. \quad (12)$$

Putting Eq. (12) into Eq. (9), we find that whereas each normal-mode k component does not acquire any additional phase upon reflection, each abnormal-mode k component gains an additional phase $\Phi_{\sigma}^{\text{abn}} = \Phi_{\sigma}^r - \Phi_{\sigma}^i \approx -2\sigma^i k_y \cot \theta_{\mathbf{k}}^i / k_0$ after reflection. Such an additional phase $\Phi_{\sigma}^{\text{abn}}$ equals the difference between the spin-redirected Berry phases possessed by the reflected and incident plane wave, and can only be nonzero in such a spin-reversal process. It can be regarded as a k_y -dependent Pancharatnam-Berry geometric phase, which originates from the spin reversal of the abnormal mode [37–39]. This kind of Pancharatnam-Berry phase is found to be intrinsic and gauge invariant [40]. Intriguingly, while the Pancharatnam-Berry phase discovered in [41–43] comes from anisotropic response of the materials, here the geometric phase results from the ‘‘effective’’ anisotropy possessed by an isotropic interface seen at oblique incidence. Based on Eqs. (9) and (12), we can easily prove that the spin-Hall shift of the abnormal mode is

$$\Delta y_{\text{abn}} = -\nabla_{k_y} \Phi_{\sigma}^{\text{abn}} = 2\sigma^i \cot \theta_{\mathbf{k}}^i / k_0, \quad (13)$$

which dictates that the momentum-dependent geometric phase gradient results in the real-space spin-Hall shift [14,40,44]. This shift is independent of optical properties of the interface.

Therefore, it is clear that only the spin-reversed abnormal mode exhibits the SHE, dictated by the geometric phase gained in the reflection process. The normal mode does not have the SHE since it does not acquire such geometric phases at all. Meanwhile, the strength of the abnormal mode, namely the Fresnel reflection coefficient under the CP bases, is sensitively dependent on the incident angle and optical properties of the interface.

We now explain the spin-Hall shifts from the perspective of angular momentum conservation [12,13,45]. Because of the rotational symmetry of the interface with respect to the z direction, the total angular momentum in this direction must be conserved. The incident circular polarization beam only has spin angular momentum (SAM) of averaged $\sigma^i \cos \theta_{\mathbf{k}}^i$ per photon in the z direction, in unit of \hbar . The z component SAMs of the normal and abnormal modes are $\sigma_{\text{nor}}^r \cos \theta_{\mathbf{k}}^r$ and $\sigma_{\text{abn}}^r \cos \theta_{\mathbf{k}}^r$, respectively, where we have $\theta_{\mathbf{k}}^r = \theta_{\mathbf{k}}^i$, $\sigma_{\text{nor}}^r = \sigma^i$, and $\sigma_{\text{abn}}^r = -\sigma^i$. Therefore, the change of the SAM in the normal mode is $\Delta L_{\text{nor}} = 0$, while that in the abnormal mode is $\Delta L_{\text{abn}} = \sigma_{\text{abn}}^r \cos \theta_{\mathbf{k}}^r - \sigma^i \cos \theta_{\mathbf{k}}^i = -2\sigma^i \cos \theta_{\mathbf{k}}^i$. This change will be converted into additional orbital angular momentum which results in the transverse spin-Hall shifts $\Delta y_{\text{nor}} = 0$ and $\Delta y_{\text{abn}} = -\Delta L_{\text{abn}} / P_x = 2\sigma^i \cot \theta_{\mathbf{k}}^i / k_0$, where $P_x = k_0 \sin \theta_{\mathbf{k}}^i$ is averaged linear momentum per photon in the x component.

This result is in good agreement with Eq. (13) based on the full-wave theory and Berry-phase analysis.

IV. RESULTS AND DISCUSSION

We now employ the formulas derived in the CP basis to reanalyze the SHE of light under LP incidences [9–12,15–17].

$$E_+^r(\mathbf{r}_\perp^r) = \int d^2\mathbf{k}_\perp^r e^{i\mathbf{k}_\perp^r \cdot \mathbf{r}_\perp^r} (M_{++} + M_{+-}) U_+^i(\mathbf{k}^i) = E_{++}^r(\mathbf{r}_\perp^r) + E_{+-}^r(\mathbf{r}_\perp^r)$$

$$E_-^r(\mathbf{r}_\perp^r) = \int d^2\mathbf{k}_\perp^r e^{i\mathbf{k}_\perp^r \cdot \mathbf{r}_\perp^r} (M_{-+} + M_{--}) U_+^i(\mathbf{k}^i) = E_{-+}^r(\mathbf{r}_\perp^r) + E_{--}^r(\mathbf{r}_\perp^r). \quad (14)$$

Obviously, Eq. (14) shows that both $E_+^r(\mathbf{r}_\perp^r)$ and $E_-^r(\mathbf{r}_\perp^r)$ are composed of a normal mode and an abnormal mode corresponding to CP incidences with different spins, as shown in Fig. 2(a). Figure 2(b) depicts how $|E_+^r(\mathbf{r}_\perp^r)|^2$ and $|E_-^r(\mathbf{r}_\perp^r)|^2$ (the field intensities of the left- and right-handed CP components inside the reflected beam) vary against the incident angle θ_K^i . The intensity patterns of two CP components change significantly as varying the incident angle, and have opposite

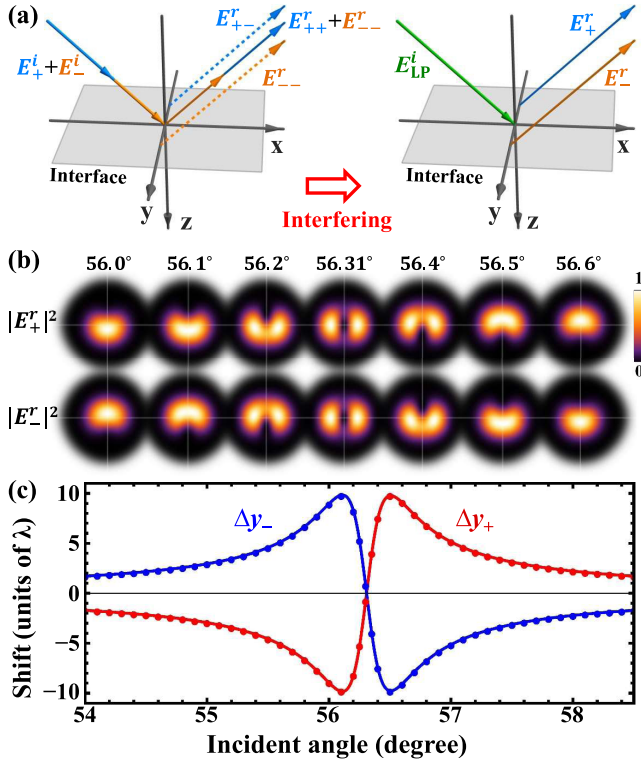


FIG. 2. Intensity distributions and spin-Hall shifts of beams reflected from the air-glass interface near the Brewster angle ($\sim 56.31^\circ$) under the illumination of a p -polarized beam. (a) Schematics of using the CP incidence results to reinterpret previous spin-Hall shifts under LP incidence. (b) Intensity distributions and (c) spin-Hall shifts of the left- and right-handed CP components of the reflected beam. The solid lines and dots separately represent rigorous results calculated by Eq. (7) and approximated ones calculated by Eq. (12). The refractive index of glass is set as 1.5, the beam waist $w_0 = 50\lambda$, and the working wavelength $\lambda = 633$ nm.

Assume that the incident beam is a p -polarized one which contains both equal-strength CP components with different spins; we get $U_+^i(\mathbf{k}^i) = U_-^i(\mathbf{k}^i)$. Put such an initial condition into Eqs. (4) and (6); we find that the CP components exhibiting different spins inside the reflected beam are

intensity evolutions. On both sides of the Brewster angle [$\theta_B = \tan^{-1}(n_2/n_1) \approx 56.31^\circ$ here], the intensity patterns exhibit opposite spin-Hall shifts, which vanish exactly at the Brewster angle [see Fig. 2(c)]. These results are consistent with those discovered in previous literature [15–17].

To judge whether the approximation [Eq. (12)] can describe well the reflection behavior at the vicinities of the Brewster angle, we calculate the spin-Hall shifts [see dots in Fig. 2(c)] with Eq. (12) and then compare them with the results obtained with the full theory [Eq. (7), solid lines in Fig. 2(c)]. They agree well with each other, which means that the Berry-phase approximation can grasp the physics of the beam reflection near the Brewster angle.

Now we are in the position to discuss the underlying mechanism of the unusual effects discussed above. Equation (14) already revealed that a CP component inside the reflected beam is a sum of two components, implying that their interference must play an important role. We take $E_+^r(\mathbf{r}_\perp^r)$ as an example to analyze the underlying mechanism. Figure 3(a) depicts how the computed spin-Hall shifts of the normal and abnormal modes vary against the incident

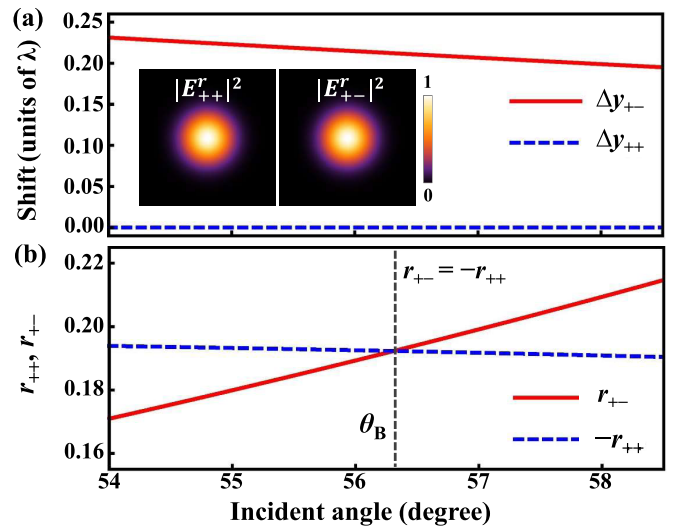


FIG. 3. Reinterpretation of the spin-Hall shift in CP basis. (a) Spin-Hall shifts of normal and abnormal modes of the reflected beam under a CP beam illumination. Inset: intensity distribution of the normal and abnormal modes. (b) Fresnel coefficients for the CP plane waves.

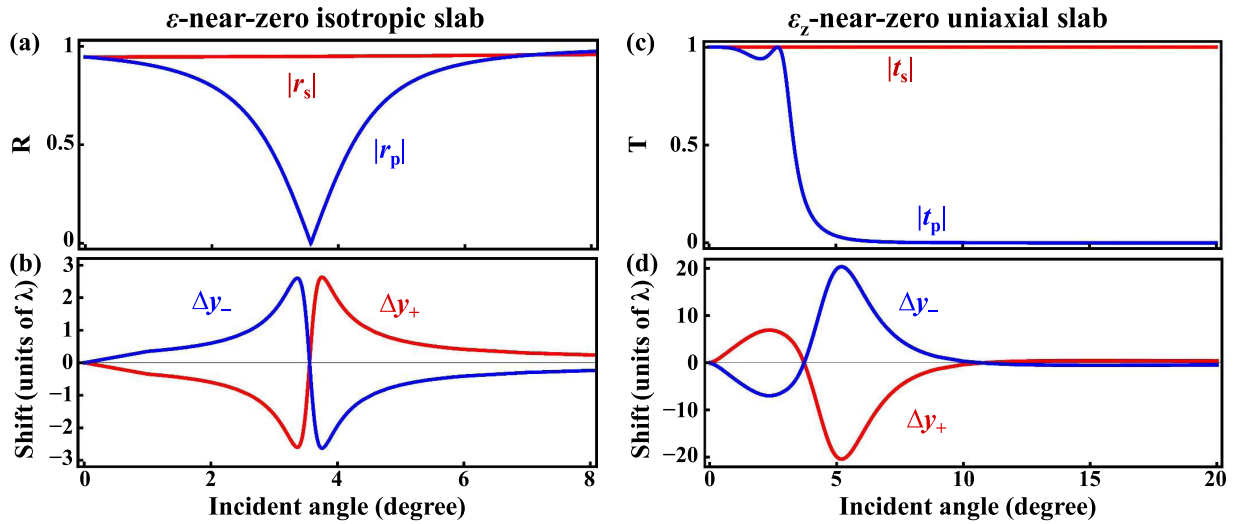


FIG. 4. Fresnel coefficients and spin-Hall shifts for two slabs placed in the free space. Left panel for an ε -near-zero slab with $\varepsilon = 0.01$ and right panel for an ε_z -near-zero uniaxial slab with $\varepsilon_x = \varepsilon_y = 1$ and $\varepsilon_z = 0.01$. Here, the slab thickness is set as $h = 1\lambda$.

near the Brewster one. The spin-Hall shifts of the normal mode are zero as expected, while those of the abnormal mode are in the order of $\lambda/5$. Meanwhile, we need to check the Fresnel coefficients (r_{++} and r_{+-}) which determine the amplitudes of two modes [see Eq. (12)]. Under the paraxial-wave approximation, we can use the Fresnel coefficients of the central wave vector \mathbf{K}^a to well approximate those of other wave components inside the incident beam. Figure 3(b) depict how the reflection coefficients r_{++} and r_{+-} of the central wave vary against the incident angle. We find that r_{++} and r_{+-} take opposite signs, and we have $r_{+-} = -r_{++}$ exactly at the Brewster angle, caused by the vanishing of reflection of the p -polarized incidence. Under such a condition, we find that the normal and abnormal modes interfere with each other destructively. Note that the two modes exhibit well-defined field patterns and that of the abnormal mode exhibit a tiny spin-Hall shift; we immediately expect that such destructive interference may generate significantly distorted final intensity pattern at the vicinities of the Brewster-angle incidence, as shown in Fig. 2(b).

V. EXTENSIONS

From the above discussion, we know that the incident angle and the optical properties of the interface are two main degrees of freedom that control the amplitude and phase of the Fresnel coefficients ($r_{++,-}$ and $r_{+,-,+}$). When the incident angle is far away from the Brewster angle, we have $r_{+,-,+} \ll r_{++,-}$ and the strength of the abnormal mode is much less than that of the normal one, making the spin-Hall shift under LP illumination very weak [15]. Therefore, if an interface can produce a Brewster-like behavior (i.e., $r_p \rightarrow 0$), we can also have $r_{+-} = -r_{++}$, and thus a giant SHE. For example, we consider an optically thin slab placed in free space, whose permittivity is near zero ($\varepsilon = 0.01$) and permeability is $\mu = 1$. Such ε -near-zero materials can be found in nature, such as indium tin oxide in the infrared range [46]. This slab exhibits Brewster-like behavior ($r_p = 0$) for light at an incident angle

of $\sim 3.57^\circ$ (see Appendix C), as shown in Fig. 4(a). In this situation, we can also expect an unusually enhanced SHE [Fig. 4(b)]. Similar Brewster-like behavior also can be found in some structured interfaces such as multilayer films [26–28], hyperbolic metamaterials [29,30], and a birefringent symmetrical metal cladding planar waveguide [31].

Our idea can be extended to the transmission cases. We note that at the air-glass interface, the spin-Hall shift of the transmitted beam under LP illumination is very small (maximum $\sim 0.1\lambda$) [11]. This is because the efficiency of the abnormal mode of the transmitted beam is very low ($t_{+,-,+} \ll t_{++,-}$). When overlapping with the normal mode, the final spin-Hall shift is very tiny. In fact, as long as the Fresnel coefficient of a designed interface has a Brewster-like behavior in the transmission ($t_p \rightarrow 0$), one can also greatly enhance the spin-Hall shift of transmitted light under LP illumination. For example, we consider a nonmagnetic ($\mu = 1$) ε_z -near-zero uniaxial slab with its optical axis being parallel to the z direction, whose permittivities are $\varepsilon_x = \varepsilon_y = 1$ and $\varepsilon_z = 0.01$. An ε_z -near-zero uniaxial slab could be realized by artificial hyperbolic metamaterial [47]. The slab is transparent for s -polarized wave ($|t_s| \equiv 1$, see Appendix C) because of $\varepsilon_x = \varepsilon_y = 1$, and totally reflects the p -polarized wave as the incident angle is larger than a critical angle ($\vartheta_c \approx 5.7^\circ$) [Fig. 4(c)] satisfying the condition of $\varepsilon_z = \sin^2 \vartheta_c$. We get, from Fig. 4(c), that the spin-Hall shift can be significantly enhanced around ϑ_c [Fig. 4(d)].

VI. CONCLUSIONS

We have reconsidered the SHE of light beams reflected at a sharp interface based on a full-wave theory. Under a CP beam illumination, the reflected beam produces a spin-reversal abnormal mode with geometric Berry phase and weak SHE, and a spin-maintained normal mode without geometric phase. We reveal that the physical origin of the geometric phase is the topological nature of the beam itself, and the efficiency of SHE is determined by the incident angle and the optical

properties of the interface. With the physical mechanism uncovered, we further demonstrate that the spin-Hall shifts of the reflected beam can be hundreds of times larger than that of the refracted beam when a p -polarized beam is reflected from a sharp interface, that is, it is the result of destructive interference of the normal and abnormal modes under the CP basis. The destructive interference leads to significant deformation of light intensity patterns and abnormally enhanced SHEs. This idea can also be extended to both reflection and transmission cases with Brewster-like behaviors. Our research clarifies the physics of the abnormally SHE near the Brewster angle and provides an alternative perspective for understanding the SHE of light.

ACKNOWLEDGMENTS

We acknowledge support from the National Natural Science Foundation of China (Grants No. 11874142 and No. 11604087), the Natural Science Foundation of Hunan Province (Grant No. 2018JJ1001), the National Key Research and Development Program of China (Grant No. 2017YFA0700202), Laboratory of Optoelectronic Control and Detection Technology of the institution of higher learning of Hunan Province.

APPENDIX A: DERIVATION OF $\phi_{\mathbf{k}}$ AND ϑ_k^a

The wave vectors of the central and an arbitrary plane wave inside a beam are denoted by \mathbf{K}^a and \mathbf{k}^a with $a = i, r, t$, re-

spectively [see Fig. 1(b)]. We define $(\hat{\mathbf{x}}, \hat{\mathbf{y}}, \hat{\mathbf{z}})$ as the laboratory coordinate system, and $(\hat{\mathbf{x}}^a, \hat{\mathbf{y}}^a, \hat{\mathbf{z}}^a)$ as the local coordinate system with $\hat{\mathbf{z}}^a \parallel \mathbf{K}^a$. Obviously, these two systems are connected by a rotation of angle $\theta_{\mathbf{K}}^a$ with respect to the y axis. Therefore, components of vector \mathbf{k}^a in different coordinate systems are connected by

$$\begin{aligned} k_x &= k_x^a \cos \theta_{\mathbf{K}}^a + k_z^a \sin \theta_{\mathbf{K}}^a \\ k_y &= k_y^a \\ k_z &= -k_x^a \sin \theta_{\mathbf{K}}^a + k_z^a \cos \theta_{\mathbf{K}}^a. \end{aligned} \quad (\text{A1})$$

\mathbf{K}^a and \mathbf{k}^a separately form angles of $\theta_{\mathbf{K}}^a$ and

$$\vartheta_k^a = \sin^{-1}(k_{\parallel}/k^a), \quad (\text{A2})$$

where $k_{\parallel} = (k_x^2 + k_y^2)^{1/2}$, with the laboratory z axis. The azimuthal angle of the incident planes of any noncentral plane wave, with respect to that of the central plane wave, reads

$$\phi_k = \tan^{-1}(k_y/k_x). \quad (\text{A3})$$

APPENDIX B: DERIVATION OF MATRIX $\mathbf{P}^{(a)}$

Based on Eqs. (1) and (4), we get the following relation for each \mathbf{k}^a component:

$$\begin{aligned} U_+^a(\mathbf{k}^a) \hat{\mathbf{V}}_+(\mathbf{K}^a) + U_-^a(\mathbf{k}^a) \hat{\mathbf{V}}_-(\mathbf{K}^a) \\ = u_+^a(\mathbf{k}^a) \hat{\mathbf{v}}_+(\mathbf{k}^a) + u_-^a(\mathbf{k}^a) \hat{\mathbf{v}}_-(\mathbf{k}^a). \end{aligned} \quad (\text{B1})$$

Multiplying both sides of Eq. (B1) by $[\hat{\mathbf{V}}_+(\mathbf{K}^a)]^*$ and $[\hat{\mathbf{V}}_-(\mathbf{K}^a)]^*$, respectively, and utilizing the orthonormal conditions, $[\hat{\mathbf{V}}_{\sigma}(\mathbf{K}^a)]^* \cdot \hat{\mathbf{V}}_{\sigma'}(\mathbf{K}^a) = \delta_{\sigma\sigma'}$, we get

$$\begin{aligned} U_+^a(\mathbf{k}^a) &= u_+^a(\mathbf{k}^a) [\hat{\mathbf{V}}_+(\mathbf{K}^a)]^* \cdot \hat{\mathbf{v}}_+(\mathbf{k}^a) + u_-^a(\mathbf{k}^a) [\hat{\mathbf{V}}_+(\mathbf{K}^a)]^* \cdot \hat{\mathbf{v}}_-(\mathbf{k}^a) \\ U_-^a(\mathbf{k}^a) &= u_+^a(\mathbf{k}^a) [\hat{\mathbf{V}}_-(\mathbf{K}^a)]^* \cdot \hat{\mathbf{v}}_+(\mathbf{k}^a) + u_-^a(\mathbf{k}^a) [\hat{\mathbf{V}}_-(\mathbf{K}^a)]^* \cdot \hat{\mathbf{v}}_-(\mathbf{k}^a), \end{aligned} \quad (\text{B2})$$

which can be simplified as the following matrix form:

$$\begin{pmatrix} U_+^a(\mathbf{k}^a) \\ U_-^a(\mathbf{k}^a) \end{pmatrix} = \mathbf{P}^{(a)} \begin{pmatrix} u_+^a(\mathbf{k}^a) \\ u_-^a(\mathbf{k}^a) \end{pmatrix} = \begin{pmatrix} [\hat{\mathbf{V}}_+(\mathbf{K}^a)]^* \cdot \hat{\mathbf{v}}_+(\mathbf{k}^a) & [\hat{\mathbf{V}}_+(\mathbf{K}^a)]^* \cdot \hat{\mathbf{v}}_-(\mathbf{k}^a) \\ [\hat{\mathbf{V}}_-(\mathbf{K}^a)]^* \cdot \hat{\mathbf{v}}_+(\mathbf{k}^a) & [\hat{\mathbf{V}}_-(\mathbf{K}^a)]^* \cdot \hat{\mathbf{v}}_-(\mathbf{k}^a) \end{pmatrix} \begin{pmatrix} u_+^a(\mathbf{k}^a) \\ u_-^a(\mathbf{k}^a) \end{pmatrix}. \quad (\text{B3})$$

Equation (B3) is just Eq. (5) in the main text.

According to Eq. (B3), we get the following explicit forms of $\mathbf{P}^{(a)}$ matrix elements through straightforward calculations:

$$P_{+-}^{(a)} = (P_{-+}^{(a)})^* = (A^+ + B^+)/2, \quad P_{-+}^{(a)} = (P_{+-}^{(a)})^* = (A^+ - B^+)/2. \quad (\text{B4})$$

With $\mathbf{P}^{(a)}$ and $\mathbf{R}(\mathbf{k}_{\parallel})$ known, we can get the $\mathbf{M}^{(r,t)}$ matrices.

APPENDIX C: FRESNEL COEFFICIENTS OF AN OPTICALLY THIN SLAB PLACED IN FREE SPACE

Consider a light beam incident on an optically thin nonmagnetic slab (thickness h , permeability $\mu = 1$, and permittivity ε), placed in the free space. The Fresnel reflection coefficients can be expressed as [1]

$$\begin{aligned} r_p(\mathbf{k}_{\parallel}) &= \frac{\left(\frac{k_z^{(2)}}{k_z^{(1)}\varepsilon} - \frac{k_z^{(1)}\varepsilon}{k_z^{(2)}}\right) \sin(k_z^{(2)}h)}{2i \cos(k_z^{(2)}h) + \left(\frac{k_z^{(1)}\varepsilon}{k_z^{(2)}} + \frac{k_z^{(2)}}{k_z^{(1)}\varepsilon}\right) \sin(k_z^{(2)}h)}, \\ r_s(\mathbf{k}_{\parallel}) &= \frac{\left(\frac{k_z^{(1)}}{k_z^{(2)}} - \frac{k_z^{(2)}}{k_z^{(1)}}\right) \sin(k_z^{(2)}h)}{2i \cos(k_z^{(2)}h) + \left(\frac{k_z^{(1)}}{k_z^{(2)}} + \frac{k_z^{(2)}}{k_z^{(1)}}\right) \sin(k_z^{(2)}h)}. \end{aligned} \quad (\text{C1})$$

Here $k_z^{(1)} = k^i \cos \vartheta_k^i$, $k_z^{(2)} = k^t \cos \vartheta_k^t$ are derived by Eq. (A2).

We then consider a nonmagnetic uniaxial slab ($\mu = 1$), placed in the free space. Its permittivity tensor is

$$\vec{\varepsilon} = \begin{pmatrix} \varepsilon_x & & \\ & \varepsilon_y & \\ & & \varepsilon_z \end{pmatrix}, \quad (\text{C2})$$

where $\varepsilon_x = \varepsilon_y \neq \varepsilon_z$. In this case the optical axis of the uniaxial slab is parallel to the laboratory z axis, that is, the system still has rotation invariance, and all the theories above are still

applicable. The transmission coefficients are given by [48]

$$t_p(\mathbf{k}_{\parallel}) = \frac{1}{\cos(q_e h) - \frac{i}{2} \left(\frac{q_e}{\varepsilon_x q_1} + \frac{\varepsilon_x q_1}{q_e} \right) \sin(q_e h)},$$

$$t_s(\mathbf{k}_{\parallel}) = \frac{1}{\cos(q_o h) - \frac{i}{2} \left(\frac{q_o}{q_1} + \frac{q_1}{q_o} \right) \sin(q_o h)}, \quad (\text{C3})$$

where $q_1 = k_0 \cos \vartheta_k^i$, $q_o = \sqrt{\varepsilon_x} k_0 \cos \vartheta_k^o$, $q_e = [\varepsilon_x k_0^2 - \frac{\varepsilon_x}{\varepsilon_z} k_{\parallel}^2]^{1/2}$, $k_{\parallel} = k_0 \sin \vartheta_k^i$, and $\vartheta_k^o = \sin^{-1}(\sin \vartheta_k^i / \sqrt{\varepsilon_x})$. The subscripts o and e respectively stand for ordinary and extraordinary. When $\varepsilon_x = \varepsilon_y = \varepsilon_z$, Eq. (C3) returns to the isotropic case. Note that the cross-polarization Fresnel coefficients between the p - and s -polarized waves are zero, because the optical axis lies in the z direction.

- [1] M. Born and E. Wolf, *Principles of Optics* (Cambridge University Press, Cambridge, UK, 1999).
- [2] D. Brewster, *Philos. Trans. R. Soc. London* **105**, 125 (1815).
- [3] Y. Fainman and J. Shamir, *Appl. Opt.* **23**, 3188 (1984).
- [4] A. Kóházi-Kis, *Opt. Commun.* **253**, 28 (2005).
- [5] A. Aiello, M. Merano, and J. P. Woerdman, *Opt. Lett.* **34**, 1207 (2009).
- [6] D. S. Citrin, *Opt. Lett.* **37**, 2376 (2012).
- [7] R. Barczyk, S. Nechayev, M. A. Butt, G. Leuchs, and P. Banzer, *Phys. Rev. A* **99**, 063820 (2019).
- [8] M. Onoda, S. Murakami, and N. Nagaosa, *Phys. Rev. Lett.* **93**, 083901 (2004).
- [9] K. Y. Bliokh and Y. P. Bliokh, *Phys. Rev. Lett.* **96**, 073903 (2006).
- [10] K. Y. Bliokh and Y. P. Bliokh, *Phys. Rev. E* **75**, 066609 (2007).
- [11] O. Hosten and P. Kwiat, *Science* **319**, 787 (2008).
- [12] K. Y. Bliokh and A. Aiello, *J. Opt.* **15**, 014001 (2013).
- [13] K. Y. Bliokh, F. J. Rodríguez-Fortuño, F. Nori, and A. V. Zayats, *Nat. Photon.* **9**, 796 (2015).
- [14] X. Ling, X. Zhou, K. Huang, Y. Liu, C.-W. Qiu, H. Luo, and S. Wen, *Rep. Prog. Phys.* **80**, 066401 (2017).
- [15] Y. Qin, Y. Li, H. He, and Q. Gong, *Opt. Lett.* **34**, 2551 (2009).
- [16] H. Luo, X. Zhou, W. Shu, S. Wen, and D. Fan, *Phys. Rev. A* **84**, 043806 (2011).
- [17] L. Kong, X. Wang, S. Li, Z. Ren, X. Wang, and H. Wang, *Appl. Phys. Lett.* **100**, 071109 (2012).
- [18] J. B. Götte, W. Löffler, and M. R. Dennis, *Phys. Rev. Lett.* **112**, 233901 (2014).
- [19] M. M. Pan, Y. Li, and J. L. Ren, *Appl. Phys. Lett.* **103**, 071106 (2013).
- [20] J. L. Ren, B. Wang, M. M. Pan, Y. F. Xiao, Q. H. Gong, and Y. Li, *Phys. Rev. A* **92**, 013839 (2015).
- [21] J. L. Ren, B. Wang, Y. Xiao, Q. Gong, and Y. Li, *Appl. Phys. Lett.* **107**, 111105 (2015).
- [22] X. Qiu, Z. Zhang, L. Xie, J. Qiu, F. Gao, and J. Du, *Opt. Lett.* **40**, 1018 (2015).
- [23] Y. Zhang, P. Li, S. Liu, L. Han, H. Cheng, and J. Zhao, *Appl. Phys. B* **122**, 184 (2016).
- [24] L. Xie, X. Zhou, X. Qiu, L. Luo, X. Liu, Z. Li, Y. He, J. Du, Z. Zhang, and D. Wang, *Opt. Express* **26**, 22934 (2018).
- [25] C. Prajapati and N. K. Viswanathan, *J. Opt.* **21**, 084002 (2019).
- [26] X. Ling, H. Luo, M. Tang, and S. Wen, *Chin. Phys. Lett.* **29**, 074209 (2012).
- [27] Y. Xiang, X. Jiang, Q. You, J. Guo, and X. Dai, *Photon. Res.* **5**, 467 (2017).
- [28] J. Li, T. Tang, L. Luo, and J. Yao, *Carbon* **134**, 293 (2018).
- [29] M. Kim, D. Lee, T. H. Kim, Y. Yang, H. J. Park, and J. Rho, *ACS Photon.* **6**, 2530 (2019).
- [30] M. Kim, D. Lee, B. Ko, and J. Rho, *APL Photon.* **5**, 066106 (2020).
- [31] H. Dai, L. Yuan, C. Yin, Z. Cao, and X. Chen, *Phys. Rev. Lett.* **124**, 053902 (2020).
- [32] X. Zhou, X. Ling, H. Luo, and S. Wen, *Appl. Phys. Lett.* **101**, 251602 (2012).
- [33] X. Qiu, X. Zhou, D. Hu, J. Du, F. Gao, Z. Zhang, and H. Luo, *Appl. Phys. Lett.* **105**, 131111 (2014).
- [34] S. Chen, X. Ling, W. Shu, H. Luo, and S. Wen, *Phys. Rev. Appl.* **13**, 014057 (2020).
- [35] R. Wang, J. Zhou, K. Zeng, S. Chen, X. Ling, W. Shu, H. Luo, and S. Wen, *APL Photon.* **5**, 016105 (2020).
- [36] W. Zhu, H. Xu, J. Pan, S. Zhang, H. Zheng, Y. Zhong, J. Yu, and Z. Chen, *Opt. Exp.* **28**, 25869 (2020).
- [37] K. Y. Bliokh, M. A. Alonso, and M. R. Dennis, *Rep. Prog. Phys.* **82**, 122401 (2019).
- [38] M. V. Berry, *Proc. R. Soc. London, Ser. A* **392**, 45 (1984).
- [39] S. Pancharatnam, *Proc. Indian Acad. Sci.: Sect. A* **44**, 247 (1956).
- [40] L.-K. Shi and J. C. W. Song, *Phys. Rev. B* **100**, 201405(R) (2019).
- [41] Z. Bomzon, V. Kleiner, and E. Hasman, *Opt. Lett.* **26**, 1424 (2001).
- [42] L. Marrucci, C. Manzo, and D. Paparo, *Phys. Rev. Lett.* **96**, 163905 (2006).
- [43] R. C. Devlin, A. Ambrosio, N. A. Rubin, J. P. B. Mueller, and F. Capasso, *Science* **358**, 896 (2017).
- [44] X. Ling, X. Zhou, X. Yi, W. Shu, Y. Liu, S. Chen, H. Luo, S. Wen, and D. Fan, *Light Sci. Appl.* **4**, e290 (2015).
- [45] S. A. Yang, H. Pan, and F. Zhang, *Phys. Rev. Lett.* **115**, 156603 (2015).
- [46] M. Z. Alam, I. De Leon, and R.W. Boyd, *Science* **352**, 795 (2016).
- [47] A. Poddubny, I. Iorsh, P. Belov, and Y. Kivshar, *Nat. Photon.* **8**, 78 (2013).
- [48] J. Lekner, *Pure Appl. Opt.* **3**, 821 (1994).